Influence of barrier suppression in high-order harmonic generation

Pablo Moreno, Luis Plaja, Victor Malyshev,* and Luis Roso
Departamento de Física Aplicada, Universidad de Salamanca, 37008 Salamanca, Spain
(Received 11 October 1994)

High-order harmonic generation accompanying photoionization presents a clear plateau structure in situations where tunneling is the fundamental process for the ejection of the electron from the core. We describe here what is expected to happen when the laser intensity is so high that barrier suppression begins to be the dominant mechanism. We show that this is an ionization regime where harmonic generation decreases with intensity, obtaining therefore an upper practical limit for high harmonic generation. Thus we are able to predict situations where the harmonic cutoff appears at a lower energy than that expected by the standard $I_P+3.17U_P$ law where I_P and U_P correspondingly are the ionization threshold for an electron in the ground state and ponderomotive energy.

PACS number(s): 32.80.Rm

I. INTRODUCTION

High-order harmonic generation accompanying ionization of atoms with very intense laser fields is, now, one of the most promising techniques to obtain coherent radiation at short wavelengths [1]. The availability of ultraintense laser sources at infrared and visible frequencies makes this region especially attractive for further study.

There are several physical mechanisms leading to harmonic generation depending on the range of frequencies and intensities of the incident laser beam. For low intensities, and for frequencies not allowing one-photon ionization, harmonic generation is essentially due to bound-bound transitions. In this regime, ionization is reached by the absorption of several photons. As the intensity increases, multiphoton ionization dominates the generation of harmonics. With a further increase of the intensity, the Keldysh parameter becomes smaller than unity, and the region of tunneling ionization is reached [2]. In this regime, the electrons ionized by tunneling and then driven by the field back to the vicinity of the core are the relevant ones to high-order harmonic generation [3–6].

The aim of this paper is to contribute to the understanding of the physical mechanisms relevant to the cutoff of the harmonic spectrum in the regime of tunneling ionization. The harmonic spectrum is usually described in terms of a plateau, or a region where the harmonic intensity is approximately independent of the harmonic order. The end of this plateau is typically very abrupt, and it is referred to as the harmonic cutoff. It is widely accepted that in this regime, a very simple expression works very well: the cutoff occurs at a frequency $\omega_{\max}\cong I_P+3.2U_P$, where $U_P=E_0^2/4\omega_L^2$ is the ponderomotive energy, I_P is the ionization threshold for an electron in the ground state, ω_L is the laser frequency, and E_0 is the electric-field amplitude. Only atomic units ($\hbar=m=e=1$) will be used in this paper. Different kinds of analytical approaches lead to this expression with slightly different coefficients, and it is confirmed by many different numerical computations. Therefore, it is considered a very good description of the end of the harmonic plateau in the tunneling regime.

Since tunneling ionization is the dominant process as the field intensity increases, it seems natural to consider whether this kind of simple expression works for arbitrary high intensities. In this paper, we want to show that this expression is valid up to the intensity where barrier suppression occurs. To show this, we compute the electron dynamics in two completely different ways. The paper includes some numerical computations of the time-dependent Schrödinger equation describing the interaction of a model atom with a linearly polarized laser field. These solutions are exact (nonperturbative), and they are compared with a simple classical model.

The results show two clear ideas. First, when the field is high enough to get into the barrier suppression regime, the cutoff energy decrease in terms of the ponderomotive energy. Second, the classical model works surprisingly well to explain the cutoff features of the quantum computation.

In the last part of the paper, we will show the comparison between the classical and quantum cutoff energies versus the amplitude of the electric field, studying the influence of the barrier suppression. The agreement between classical and quantum calculations is also remarkable for the prediction of the cutoff energy of the high-order harmonic spectrum. From the numerical results, we get the same qualitative behavior: a significant decrease in the cutoff energies from a certain value of the field. This clarifies the widely accepted feeling that very high intensities are not useful for the generation of high-order harmonics, as indicated by the numerical studies of harmonic generation just before the intensity is strong enough to enter the adiabatic stabilization regime.

II. TIME-DEPENDENT SCHRÖDINGER EQUATION

We consider a typical one-dimensional quantum model that only studies the dynamics along the polarization axis

*Permanent address: Research Center, Vavilov State Optical Institute, 199034 St. Petersburg, Russia.

of the laser field. The time-dependent Schrödinger equation, in the $\vec{A}\cdot\vec{p}$ gauge, is

$$i\frac{\partial}{\partial t}\varphi(z,t)=-\frac{1}{2}\frac{\partial^2}{\partial z^2}\varphi(z,t)-\frac{1}{\sqrt{z^2+1}}\varphi(z,t)$$
$$-\frac{i}{c}A_0\cos(\omega_L t)\frac{\partial}{\partial z}\varphi(z,t)\ . \quad (1)$$

A_0 is the vector potential, polarized along the z direction. The electric field is, therefore, $E_0\sin(\omega_L t)$, where $E_0=\omega_L A_0/c$.

This model is widely accepted to include most of the essential features of the ionization dynamics, specially in the strong-field regime, because in this case the electron moves mostly along the polarization axis. The Coulomb atomic potential is given by the standard expression with the square root in the denominator. Of course, this simple one-dimensional model does not include angular momentum. It is well known that it allows eigenstates with parity as a good quantum number. Therefore, the laser field induces transitions between even and odd states. The ground state of this model atom has an energy $I_P=0.67$ a.u., and the excited states form an infinite series of even and odd bound states completely similar to the Rydberg series in three-dimensional hydrogen [7].

We calculate the harmonic spectrum by Fourier transforming the time-dependent acceleration, $\ddot{d}(t)=\langle\varphi(z,t)|-dV/dz|\varphi(z,t)\rangle$ [8], where V is the one-dimensional Coulomb atomic potential used in Eq. (1) and the dots indicate the time derivatives. In this expression, for simplicity, the contribution of the incident field to the fundamental component has been omitted. We will refer to harmonic spectrum to indicate the square modulus of this transform, $|\ddot{d}(\omega)|^2$.

III. NUMERICAL RESULTS

We have performed the numerical solution of the time-dependent Schrödinger equation (1) for the case of tunneling ionization. We have chosen for the computations the following laser frequency, $\omega_L=0.06$ a.u., which corresponds to a 12-photon ionization process from the unperturbed ground state. This is a typical multiphoton order suitable for comparison with the experiments in noble gases. For the computations shown here, a linear turn on of two cycles has been chosen.

A typical harmonic spectrum, computed for $\omega_L=0.06$ a.u., and an electric-field amplitude $E_0=0.1$ a.u. is shown in Fig. 1. This harmonic spectrum presents the well-known plateau structure with a cutoff according to the $3.17U_P$ law. For these parameters, this law predicts the

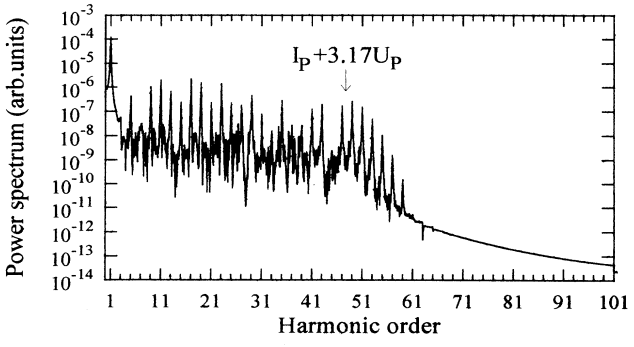

FIG. 1. A typical high-order harmonic spectrum, calculated from the numerical solution of the one-dimensional Schrödinger equation for an electric-field amplitude $E_0=0.1$ a.u. and a laser frequency $\omega_L=0.06$ a.u. This harmonic spectrum presents the well-known plateau structure with a cutoff according to the $3.17U_P$ law (indicated by the vertical arrow). The pulse has a duration of five optical cycles, two cycles of turn on (as a linear ramp) and three cycles of constant amplitude.

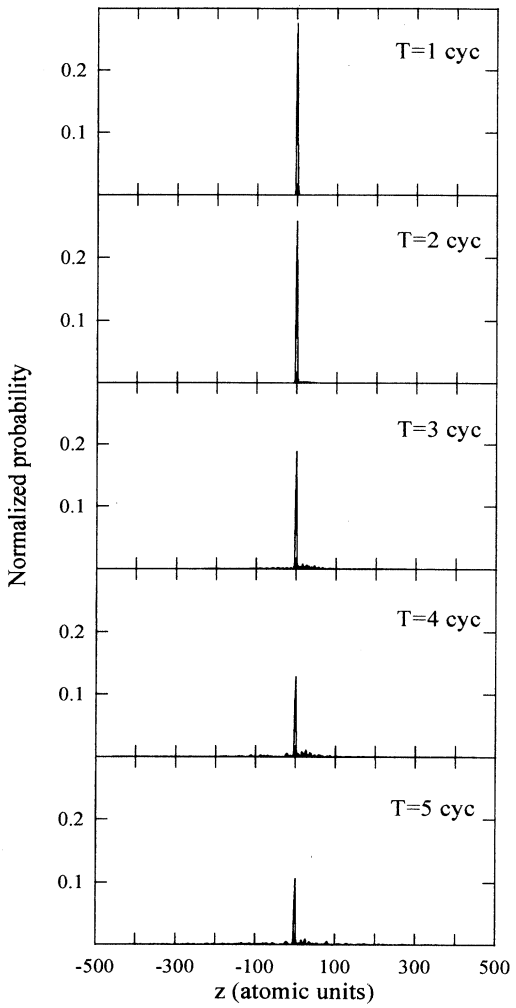

FIG. 2. Spatial distribution of the electron density $|\varphi(z,t)|^2$ as a function of the space coordinate z for different values of the time: $t=1$, 2, 3, 4, and 5 cycles. These snapshots show a typical electron cloud under ionization, where some part undergoes tunneling ionization and some other part remains close to the nucleus. The drawings represent the numerical solution of the one-dimensional Schrödinger equation for an electric-field amplitude $E_0=0.1$ a.u., and a laser frequency $\omega_L=0.06$ a.u. The pulse has a duration of five optical cycles, two cycles of turn on (as a linear ramp) and three cycles of constant amplitude. Some population remains not ionized.

cutoff at $\omega_{max}=2.2$ a.u., which approximately corresponds to the 49th harmonic of the incident frequency ω_L (indicated by the vertical arrow in the figure).

It is well known that, at low frequencies, multiphoton ionization and tunneling ionization are two competing processes [2]. Their relative importance is given by the Keldysh parameter γ defined as

$$\gamma=\left[\frac{I_P}{2U_P}\right]^{1/2}=\frac{\omega_L}{E_0}\sqrt{2I_P}\ , \tag{2}$$

where, as indicated before, U_P is the ponderomotive energy and $I_P=0.67$ a.u. is the ionization threshold for an electron in the ground state. For these parameters, $\gamma=0.7$. The fact that the Keldysh parameter is small ($\gamma<1$) indicates that tunneling is the dominant mechanism of ionization, and it will also be dominant for higher fields.

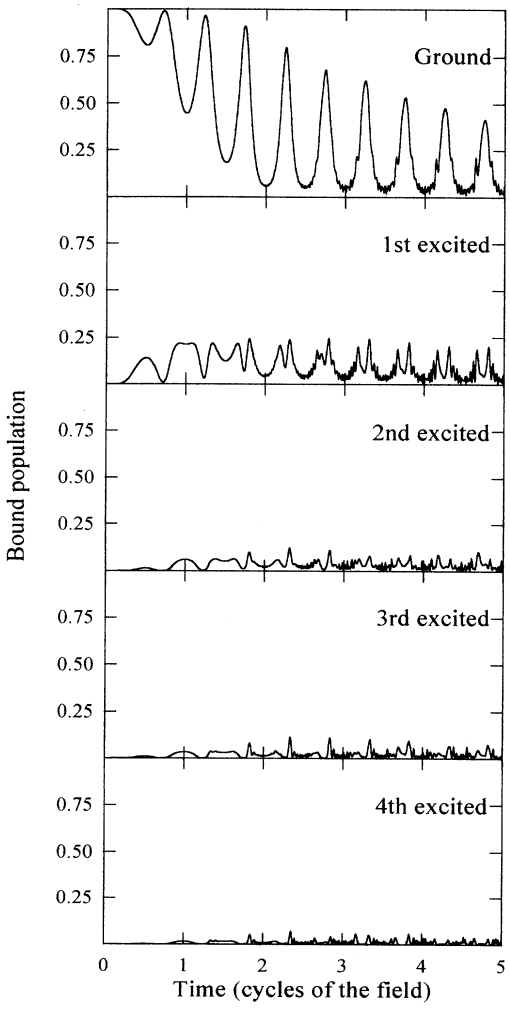

FIG. 3. Time distribution of the population of the lowest bound states, computed from the numerical solution of the one-dimensional Schrödinger equation for an electric field amplitude $E_0=0.1$ a.u. and a laser frequency $\omega_L=0.06$ a.u. The pulse has a duration of five optical cycles, two cycles of turn on (as a linear ramp) and three cycles of constant amplitude.

The time evolution of the electron wave function for the same parameters as in Fig. 1 is shown in Figs. 2 and 3. Figure 2 represents some snapshots of the wave function for each cycle of the field. These computations show a typical electron cloud under ionization. Part of the wave packet remains bound—with a sharp peak at $z=0$—and the rest spreads over a wide region of the space. Figure 3 represents the time evolution of the ground state and the first few excited bound states. The evolution of the wave packet evidences that the electron goes through the nucleus in its oscillation. These dynamics suggest that some features of the motion of the electron can be understood with a classical model, although this comparison is not direct, therefore, it is worth exploring deeply the classical ideas.

IV. CLASSICAL EXPLANATION

Tunneling ionization is essentially a quantum process. However, just after ionization, it is reasonable to consider the free electron as a classical particle. In this case, the motion of the electron is given by the well-known equations,

$$\begin{aligned}\ddot{z}(t)&=-E_0\sin(\omega_L t+\zeta)\ ,\\ \dot{z}(t)&=\dot{z}_0+\frac{E_0}{\omega_L}[-\cos\zeta+\cos(\omega_L t+\zeta)]\ ,\\ z(t)&=z_0+\dot{z}_0 t+\frac{E_0}{\omega_L^2}[-\omega_L t\cos\zeta+\sin(\omega_L t+\zeta)-\sin\zeta]\ ,\end{aligned} \tag{3}$$

where ζ is the phase of the electric field just at the tunneling ionization moment. This phase can take any value because it refers to our lack of knowledge about the exact moment in which this electron is released from the nucleus. From these equations, it is clear that the phase ζ is responsible for the drift velocity of the electron in the laser field,

$$v_{\text{drift}}=\dot{z}_0-\frac{E_0}{\omega_L}\cos\zeta\ . \tag{4}$$

We will set $\dot{z}_0$ equal to zero, provided the probability of tunneling ionization depends on the momentum of the ejected electron and this probability is maximum for zero momentum [2]. The initial position z_0 is the distance at which the electron is released. As the tunneling probability depends also on the width of the effective potential barrier, the most likely mechanism is that the electron is released close to the nucleus. For the situation in which we are interested, of large classical excursions of the freed electron, this is practically equivalent to consider $z_0=0$.

It has been shown in earlier works [3,5] that the maximum kinetic energy of an electron ionized by the tunnel effect and coming back to the nucleus is $3.17U_P$. This energy is released as the electron is captured again by the nucleus giving rise to harmonic spectrum extended until the order corresponding to an energy of $I_P+3.17U_P$. Therefore, this recombination of the electron is only possible in the vicinity of the nucleus, and it is reasonable to consider that it happens at $z=0$, provided the large ex-

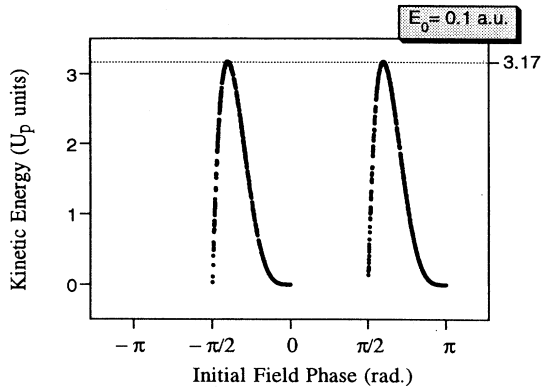

FIG. 4. Classical kinetic energies of an electron ionized by tunneling that comes back to the nucleus, plotted versus the phase of the field at tunneling. This figure corresponds to an electric-field amplitude $E_0=0.1$ a.u. and a laser frequency $\omega_L=0.06$ a.u. There is a region of initial phases where the electrons never come back to the nucleus. The density of the small dots that constitute these curves is an indication of the density of classical trajectories. The horizontal solid line corresponds to 3.17 times the ponderomotive energy and is the absolute maximum of the kinetic energy for the classical trajectories that start from the origin, with zero velocity, and come back to the nucleus. The pulse has a duration of five optical cycles, two cycles of turn on (as a linear ramp) and three cycles of constant amplitude.

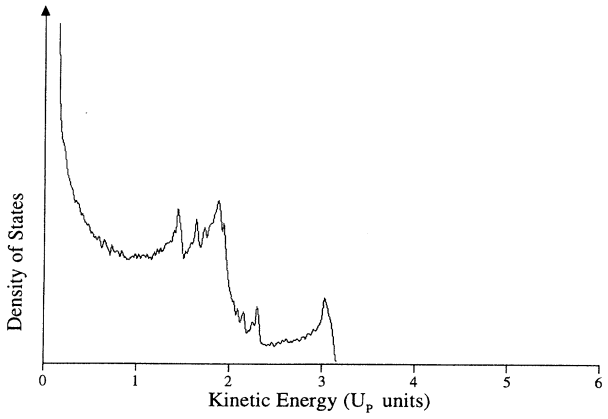

FIG. 5. Distribution of kinetic energies of the classical electron trajectories coming back to the nucleus. For different values of the tunneling phase, we have plotted the density of trajectories that return to the nucleus. This figure corresponds to an electric-field amplitude $E_0=0.1$ a.u. and a laser frequency $\omega_L=0.06$ a.u., although this profile is quite general for a broad range of parameters. The peak at 3.17 times the ponderomotive energy is the absolute maximum value of the kinetic energy back to the nucleus. There are other peaks in the classical density of trajectories, for example at twice the ponderomotive energy, that correspond to trajectories that cross many times over the nucleus.

cursion of the electron in these intense fields.

However, a very small range of values for the phase ζ contributes to this maximum value of the kinetic energy. The rest of the phases contribute to other values of the kinetic energy for the electron that comes back to the nucleus. In Fig. 4, we have plotted the kinetic energy of the electron when it comes back to the nucleus, following a classical trajectory, as a function of the initial phase, i.e., as a function of the moment when the electron was released. This figure corresponds to an electric-field amplitude $E_0=0.1$ a.u., and a laser frequency $\omega_L=0.06$ a.u. There is a region of initial phases where the electrons never come back to the nucleus. The density of the small dots that constitute this curve is an indication of the density of classical trajectories. The horizontal solid line corresponds to $3.17U_P$, which is the maximum value of the kinetic energy of a classical electron that starts moving from the origin, with zero velocity, and returns to the nucleus.

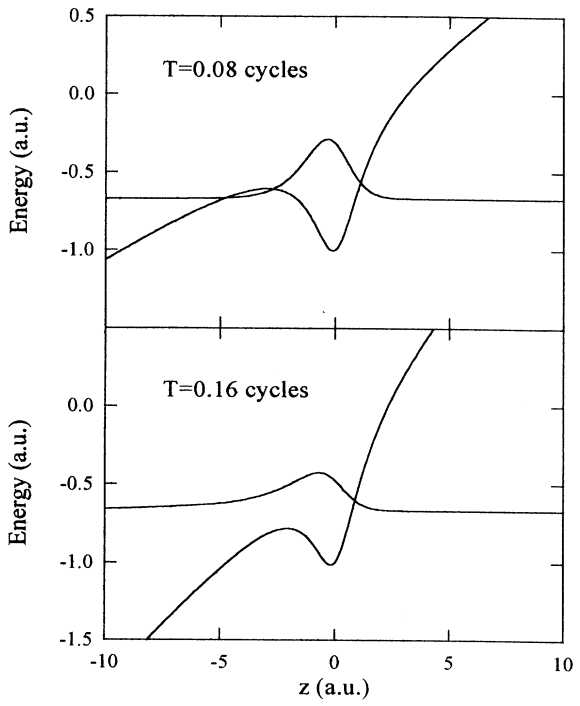

FIG. 6. This is the quasistatic potential that the electron feels. The laser field amplitude is $E_0=0.2$ a.u. Drawing (a) corresponds to the instantaneous electric field at time equal to 0.08 cycles. For this phase, the electron needs to tunnel across the potential barrier to be ionized. Drawing (b) corresponds to an instantaneous electric field at time equal to 0.16 cycles. For this last value of the phase, the potential barrier is suppressed for an electron initially at the ground state. The time-dependent wave function is also plotted, showing how the electrons begin to leave the atom after the barrier suppression.

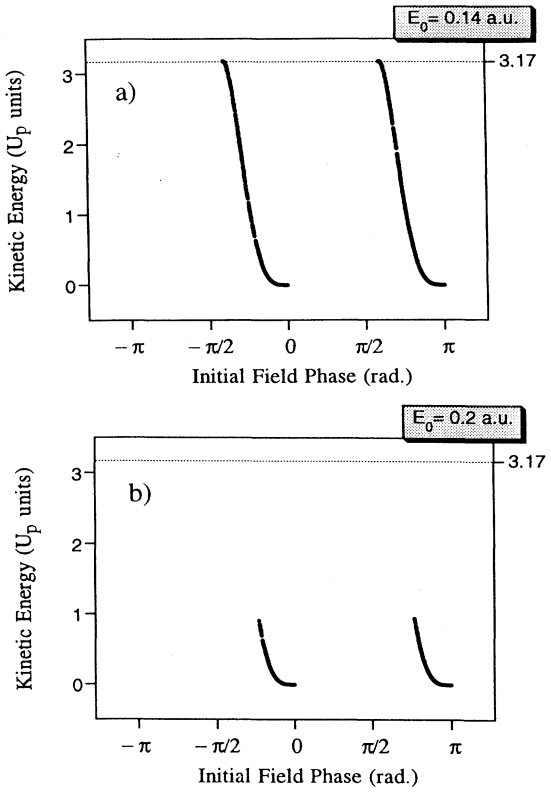

FIG. 7. Classical kinetic energies of an electron ionized by tunneling that comes back to the nucleus, plotted versus the phase of the field at the tunneling instant. This figure is analogous to Fig. 4, with the same laser frequency, $\omega_L=0.06$ a.u. However, the electric-field amplitude now is (a) $E_0=0.14$ a.u. and (b) $E_0=0.2$ a.u. The first value has been chosen because it is very close to the critical value $E_C=0.1337$ a.u. This figure still shows the maximum kinetic energy of 3.17 times the ponderomotive energy. The second value is high enough to satisfy the barrier suppression condition. Just after the barrier suppression most of the electron population is directly ionized, therefore, these phases are absent in the drawing and the maximum kinetic energy is reduced.

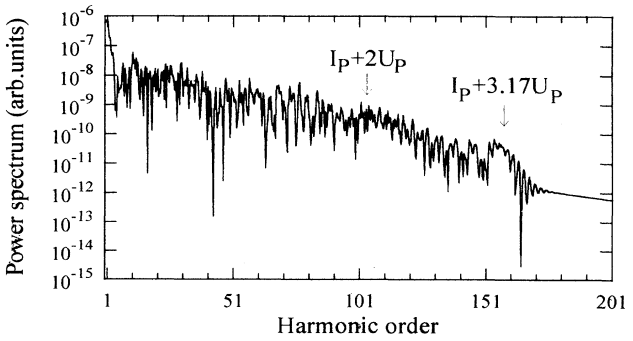

FIG. 8. A typical high-order harmonic spectrum calculated from the numerical solution of the one-dimensional Schrödinger equation for an electric-field amplitude $E_0=0.2$ a.u. and a laser frequency $\omega_L=0.06$ a.u. In contrast to Fig. 1, now barrier suppression begins to play a role. The arrow indicates that $3.17U_P$ law. The pulse has a duration of five optical cycles, two cycles of turn on (as a linear ramp) and three cycles of constant amplitude.

We can get more information about the classical trajectories by studying the distribution of the kinetic energies at the moment the electron comes back to the nucleus, as depicted in Fig. 5. In contrast to the previous figure, we have followed now the classical trajectory of the electron for many cycles, rather than limiting to the first trajectory coming back to the nucleus. Therefore, in this picture, the relative importance of the trajectories with very slow drift velocity is accentuated because they pass many times over the nucleus. This figure corresponds to an electric-field amplitude $E_0=0.1$ a.u., and a laser frequency $\omega_L=0.06$ a.u., although this profile is quite general for a broad range of parameters. The peak at 3.17 times the ponderomotive energy is the absolute maximum value of the kinetic energy of an electron returning to the nucleus. This trajectory corresponds to $\zeta_{\max}=1.88+n\pi$, for any positive integer n. This means that it is completely impossible—regardless of the initial phase—to have a classical trajectory starting from the nucleus ($z_0=0$) without initial velocity ($\dot{z}_0=0$) and coming back to the nucleus with a kinetic energy higher than $3.17U_P$ when it passes again over $z=0$. This maximum corresponds to a one-pass trajectory. Other peaks in the density of classical trajectories correspond to those trajectories with many passages through the nucleus. In particular, from Eq. (4) a periodic trajectory is obtained from $z_0=0$, $\dot{z}_0=0$, which passes over the nucleus with energy $2U_P$. This periodic trajectory corresponds to $\zeta=\pi/2$, i.e., to electrons emitted when the electric field is just at its maximum. For initial phases very close (but not exactly equal) to this value, the drift motion is very small compared to the quiver motion and the electron is able to pass over the nucleus many times with kinetic energies close to $2U_P$.

V. BARRIER SUPPRESSION

We have shown so far a qualitative agreement between the quantum computations and the classical model, in the

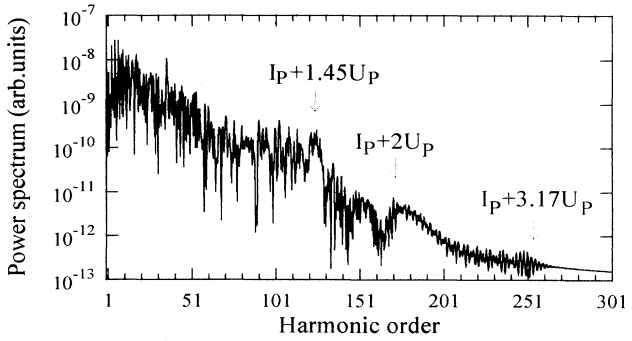

FIG. 9. A typical high-order harmonic spectrum calculated from the numerical solution of the one-dimensional Schrödinger equation for a stronger electric field $E_0=0.3$ a.u. than in Fig. 8, and a laser frequency $\omega_L=0.06$ a.u. The pulse has a duration of five optical cycles, two cycles of turn on (as a linear ramp) and three cycles of constant amplitude. Now barrier suppression is more important, and the $3.17U_P$ law (indicated by the vertical arrow) gives only the end of a very weak plateau, being the end of the most important plateaus at $2U_P$ and $1.45U_P$.

tunneling regime. At higher field intensities, as the amplitude of the electric field increases, an unexpected feature appears in the spectra: the cutoff energy becomes lower than $I_P+3.17U_P$. If the field is high enough, the effective potential (i.e., Coulomb plus field) can be distorted in such a way that no bound state is present (Fig. 6). We know that the electrons that recombine with the nucleus producing the highest harmonic orders are precisely those that have tunneled to the continuum when the field was close to its maximum. For higher fields, these electrons have already been released before the field reaches this maximum value, and consequently, their maximum kinetic energy coming back to the nucleus is smaller.

In the classical picture, this means a restriction in the initial phase to satisfy the condition $E_C \geq E_0 \sin\zeta$, where E_C is the critical field corresponding to the complete potential barrier suppression (i.e., no minimum is present). In this last part of this paper, we want to show the comparison between the classical and quantum cutoff energies versus the amplitude of the electric field. Of course, the classical simulation does not allow one to explain more than some qualitative features of the harmonic cutoff behavior.

Figure 7 shows the classical kinetic energies of an electron ionized by tunneling that comes back to the nucleus, plotted versus the phase of the field at the moment of tunneling. This figure is analogous to Fig. 4, with the same laser frequency, $\omega_L=0.06$ a.u. However, the electric-field amplitude now is (a) $E_0=0.14$ a.u. and (b) $E_0=0.17$ a.u. The first value has been chosen because it is very close to the critical value $E_C=0.1337$ a.u. This figure still shows electron trajectories reaching the maximum

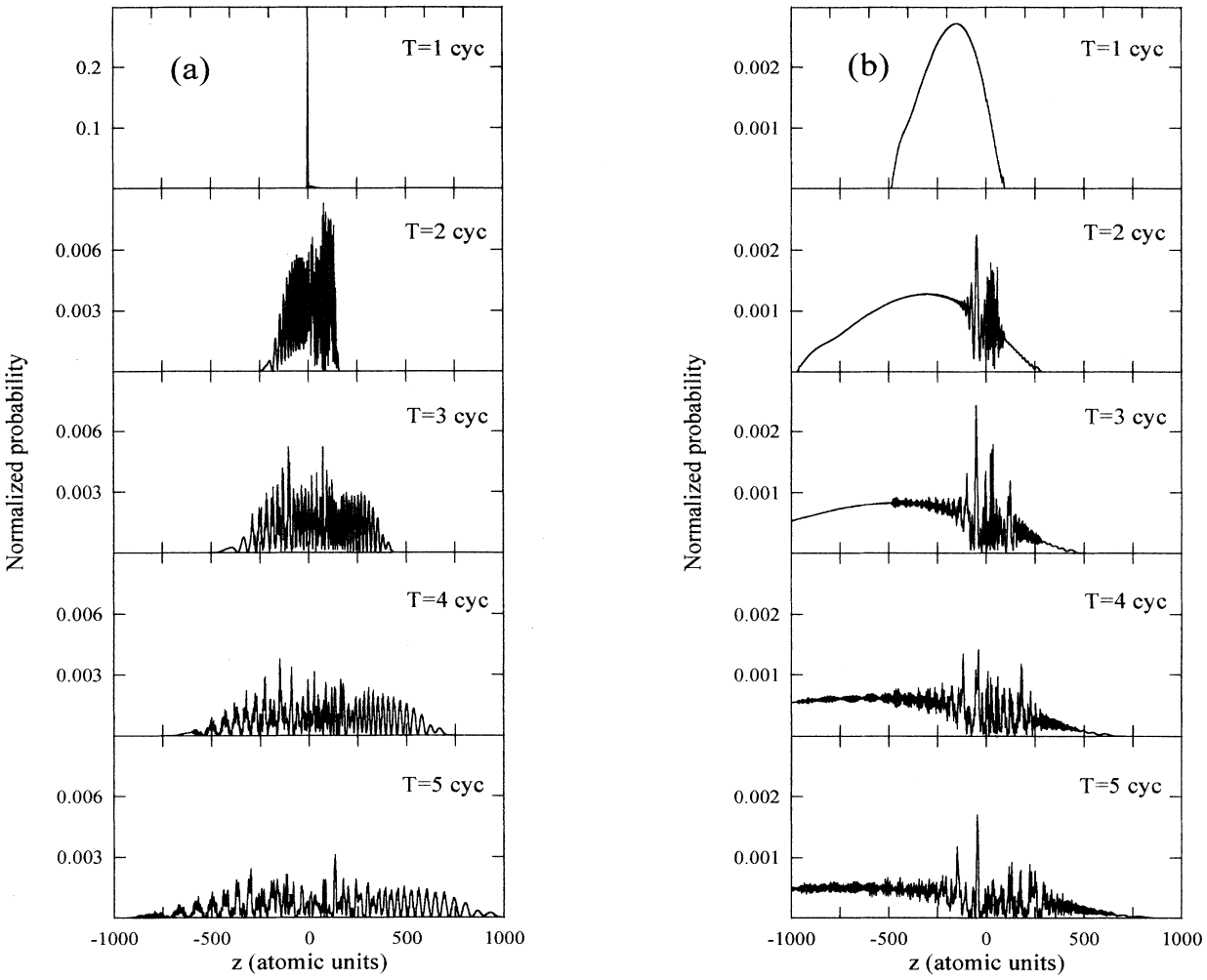

FIG. 10. Spatial distribution of the electron density $|\varphi(z,t)|^2$ as a function of the space coordinate z for different values of the time $t=0$, 1, 2, 3, 4, and 5 optical cycles. These snapshots show a typical electron cloud under ionization in a situation where barrier suppression gives rise to a clear wave packet. The drawings represent the numerical solution of the one-dimensional Schrödinger equation for an electric-field amplitude $E_0=0.2$ a.u. and a laser frequency $\omega_L=0.06$ a.u. Figure 10(a) corresponds to two cycles of turn on (as a linear ramp) and three cycles of constant amplitude. In this case there is not drift motion of the center of the wave packet. In comparison to the classical calculations, Fig. 10(b) corresponds to a square pulse. Now the center of the wave packet has a drift velocity.

kinetic energy of 3.17 times the ponderomotive energy. The second value is high enough to satisfy the barrier suppression condition, and there are no trajectories coming back to the nucleus with kinetic energies higher than twice the ponderomotive energy. Just after the barrier suppression, most of the electron population is directly ionized, therefore, these phases are absent in the drawing.

This prediction of the semiclassical model is confirmed by the numerical computations of the time-dependent Schrödinger equation. Figure 8 shows the high-order harmonic spectrum calculated for an electric-field amplitude $E_0=0.2$ a.u., and a laser frequency $\omega_L=0.06$ a.u. Now barrier suppression begins to play an important role, and the $3.17U_P$ law (indicated by the vertical arrow) gives only the end of a secondary plateau. However, this is more evident as the laser amplitude is increased, as shown in Fig. 9, corresponding to a stronger electric field, $E_0=0.3$ a.u., than in Fig. 8, and the same laser frequency

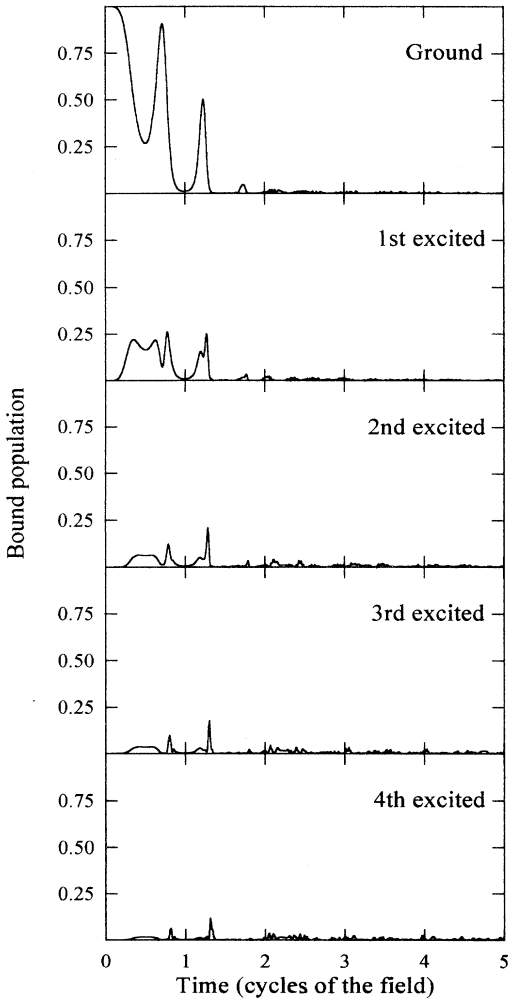

FIG. 11. Time distribution of the population of the ground state, computed from the numerical solution of the one-dimensional Schrödinger equation for an electric-field amplitude $E_0=0.2$ a.u. and a laser frequency $\omega_L=0.06$ a.u. The pulse has a duration of five optical cycles, two cycles of turn on (as a linear ramp) and three cycles of constant amplitude.

$\omega_L=0.06$ a.u. Now barrier suppression is even more important, being the end of one plateau at $2U_P$ associated with some classical periodic trajectories of electrons ionized during the turn on, when the maximum amplitude of the field is smaller than the final value E_0. Since they have a small drift velocity, they interact with the nucleus for longer times. Another plateau arriving until $1.45U_P$ reflects the elimination, due to the suppression of the barrier, of those initial phases that contribute to the most energetic returning trajectories of the electron.

The time evolution of the electron wave function for the same parameters as in Fig. 8 is shown in Figs. 10 and 11. Figure 10 represents some snapshots of the wave function for each cycle of the field. Figure 11 represents the time evolution of the ground state, showing a very clear electron wave packet that goes through the nucleus in its oscillations. These dynamics explain why some qualitative features of the electron motion can be understood with the classical model.

It is clear from these numerical computations that several plateaus are present in the high-order harmonic spectra at different intensities. We can study them in a continuous way as a function of the laser field amplitude E_0. Figure 12 shows the cutoff frequency (in U_P units) as a function of the laser field amplitude (for a laser frequency $\omega_L=0.06$ a.u.). As the electric field increases, barrier suppression begins to play a fundamental role and different plateaus disappear because they correspond to classical trajectories with no allowed initial phases, assuming that just after barrier suppression, all electrons are ionized. From these numerical results, we get a significant decrease in the cutoff energies (measured in U_P units) starting from values of the field where barrier suppression is possible, according to the classical model prediction. The exact details of these secondary plateaus cannot be explained with the classical model, because

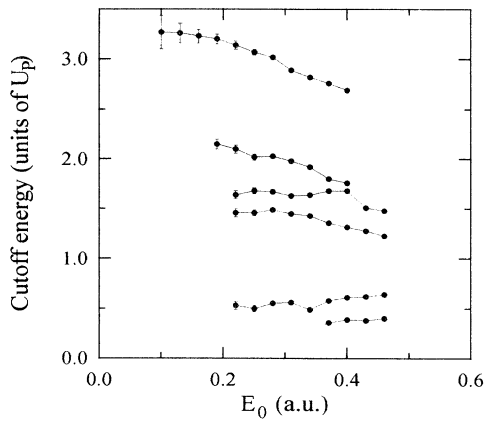

FIG. 12. Several plateaus are present in the high-order harmonic spectra at different intensities. The figure shows the cutoff frequency (in U_P units) as a function of the laser field amplitude for a laser frequency $\omega_L=0.06$ a.u. As the electric field increases, barrier suppression begins to play a fundamental role and different plateaus disappear because they correspond to classical trajectories with initial phases not allowed assuming that just after barrier suppression all electrons are ionized.

they probably include effects of electron wave-function interference. However, we consider that the physical origin of the disappearance of the most energetic harmonics is due to the elimination of the initial phases responsible for some returning trajectories of the electron.

VI. CONCLUSION

We have shown that a lot of physical insight can be obtained with a preliminary use of classical electron trajectories. Of course, the fine details should be calculated with the use of the time-dependent Schrödinger equation.

Applying this idea to a situation involving barrier suppression, we have clearly identified the mechanism that prevents the expansion of the harmonic plateau according to the $I_P+3.17U_P$ law. In fact, the classical model predicts a shrinking of the plateau in the barrier suppression regime that is more and more pronounced as the field increases. This plateau shrinking effect has been also seen in the quantum simulations.

These conclusions can be applied to different situations because barrier suppression is independent of the laser frequency. One of these situations is the adiabatic stabilization, where numerical simulations also show very narrow plateaus, for intensities well beyond the critical field, and frequencies corresponding to one-photon ionization.

ACKNOWLEDGMENTS

Support from the Spanish Dirección General de Investigación Científica y Tecnológica (under Grants No. PB-92-0600-C03-03 and No. PB-93-0632) and from the European Union Human Capital and Mobility Program (under Contracts No. CHRX-CT93-0346 and No. CHRX-CT94-0470) is acknowledged. One of the authors. (V.M.) also acknowledges the Universidad de Salamanca for a visitor position.

[1] See, for example, *Super-Intense Laser-Atom Physics,* edited by Bernard Piraux, Anne L'Huillier, and Kazimierz Rzazewski (Plenum, New York, 1993).

[2] S. Augst, D. Strickland, D. D. Meyerhofer, S. L. Chin, and J. H. Eberly, Phys. Rev. Lett. **63**, 2212 (1989); a recent review of photoionization physics, including tunneling physics, can be found in N. B. Delone and V. P. Krainov, *Multiphoton Processes in Atoms,* Vol. 13 of Springer Series on Atoms and Plasmas, edited by G. Ecker, P. Lambropoulos, I. I. Sobel'man, and H. Walther (Springer-Verlag, Berlin, 1993).

[3] P. B. Corkum, Phys. Rev. Lett. **71**, 1994 (1993).

[4] K. J. Schafer, B. Yang, L. F. DiMauro, and K. C. Kulander, Phys. Rev. Lett. **11**, 1599 (1993).

[5] J. L. Krause, K. J. Schafer, and K. C. Kulander, Phys. Rev. A **45**, 4998 (1992).

[6] S. Geltman, J. Phys. B **27**, 1497 (1994).

[7] Q. Su and J. H. Eberly, Phys. Rev. A **44**, 5997 (1991).

[8] V. C. Reed and K. Burnett, Phys. Rev. A **46**, 424 (1992).